

Article

NC-OFDM Satellite Communication Based on Compressed Spectrum Sensing

Yong Wang ^{1,2}, Hehao Niu ^{1,2} , Qingsong Zhao ^{1,2}, Lei Wang ^{1,2}, Yue Gao ³ and Zhi Lin ^{1,2,*}

¹ College of Electronic Countermeasure, National University of Defence Technology, Hefei 230037, China; wyeei@126.com (Y.W.); niuhaonupt@foxmail.com (H.N.); pine_zhao@yeah.net (Q.Z.); wanghfe@163.com (L.W.)

² Anhui Province Key Laboratory of Electronic Restriction, Hefei 230037, China

³ School of Computer Science, Fudan University, Shanghai 200433, China; gao_yue@fudan.edu.cn

* Correspondence: linzhi@nudt.edu.cn

Abstract: With the fast development of giant LEO constellations, the effective spectrum utilization has been regarded as one of the key orientations for satellite communications. This paper focuses on improving the spectrum utilization efficiency of satellite communications by proposing a non-continuous orthogonal frequency division multiplexing (NC-OFDM) method. Based on the models of NC-OFDM system, we first propose a sub-carrier allocation method by using spectrum sensing to efficiently perceive and utilize the spectrum holes in the satellite communication system. Then, a hybrid genetic particle swarm optimization method is adopted to allocate the channel resources effectively. Finally, simulation results verify that the proposed algorithm can significantly improve the spectrum efficiency of satellite communications.

Keywords: NC-OFDM; satellite communications; compressed spectrum; hybrid genetic algorithm particle swarm optimization



Citation: Wang, Y.; Niu, H.; Zhao, Q.; Wang, L.; Gao, Y.; Lin, Z. NC-OFDM Satellite Communication Based on Compressed Spectrum Sensing. *Sensors* **2022**, *22*, 3800. <https://doi.org/10.3390/s22103800>

Academic Editor: Mario Marchese

Received: 13 April 2022

Accepted: 12 May 2022

Published: 17 May 2022

Publisher's Note: MDPI stays neutral with regard to jurisdictional claims in published maps and institutional affiliations.



Copyright: © 2022 by the authors. Licensee MDPI, Basel, Switzerland. This article is an open access article distributed under the terms and conditions of the Creative Commons Attribution (CC BY) license (<https://creativecommons.org/licenses/by/4.0/>).

1. Introduction

Recently, cognitive radio technology has been regarded as a promising solution for solving spectrum resource shortages due to its characteristic of efficient spectrum utilization [1–3]. In addition, satellite communications have received significant attention due to their widely applicability in emergency rescues, environmental monitoring, and network access in unpopulated areas [4–12]. The spectrum management of most commercial geostationary orbit communication satellites follows fixed channel authorization allocation modes. With the increase in message volume and the number of users, the frequency band is becoming more and more crowded, and the spectrum resources are increasingly scarce. However, satellite communication channels are not occupied by users all the time, resulting in a large number of spectrum holes in the spectrum of satellite communication. In a report written by the Spectrum Policy Task Force [13], the FCC noted that the spectrum utilization in the vast majority of the authorized spectrum allocated is only 15 to 85%. The report points out the prominent contradictions in spectrum management: spectrum resources are scarce, but the spectrum utilization rate is very low.

NC-OFDM uses cognitive radio technology to discover the spectrum holes in the communication environment and to obtain access to them in the form of non-continuous subcarriers, which avoids the interference from cognitive users to authorized users [14,15]. Other multiple access methods, such as spread spectrum, cannot use spectrum holes due to their continuous spectrum characteristics. The NC-OFDM-related research mainly focuses on spectrum forming [16], channel estimation [17], synchronous [18], peak ratio suppression [19], etc., but there is no detailed solution for NC-OFDM satellite communication proposed. OFDM technology is proposed to be applied to the field of satellite communication, and OFDM communication satellites will be developed [20,21]. Recently,

in [22], the authors proposed using NC-OFDM in satellite communication to improve the spectrum efficiency. However, the cost of launching OFDM communication satellites is high. An NC-OFDM system based on cognitive radio can achieve spectrum sharing with authorized users, so it can greatly improve the spectrum utilization. If NC-OFDM can be combined with satellite communication, the spectrum utilization efficiency of satellite communication will be greatly improved, and the shortage of spectrum resources will be alleviated.

The most valuable resource in wireless communication is frequency spectrum, and the rational utilization, sharing, and protection of the radio spectrum has become a growing requirement. It is obviously an economical and feasible means to apply NC-OFDM to satellite communication, which will improve the spectrum utilization efficiency of satellite communication.

2. NC-OFDM Satellite Communication System Model Based on Spectrum Sensing

The NC-OFDM satellite communication system based on cognitive radio is a new type of communication system. In addition to the non-continuous subcarrier functions and the up-and-downlink data transmission functions of satellite communication systems, a spectrum-sensing module is specifically designed. This module can panoramically perceive the spectrum usage of communication satellites and detect spectrum holes. It reasonably allocates non-continuous subcarriers according to the number and frequency band range of the spectrum holes, and sends the dynamic subcarrier allocation scheme to the subcarrier control module in real time for spectrum forming. The basic model of the transmission and reception system is shown in Figure 1.

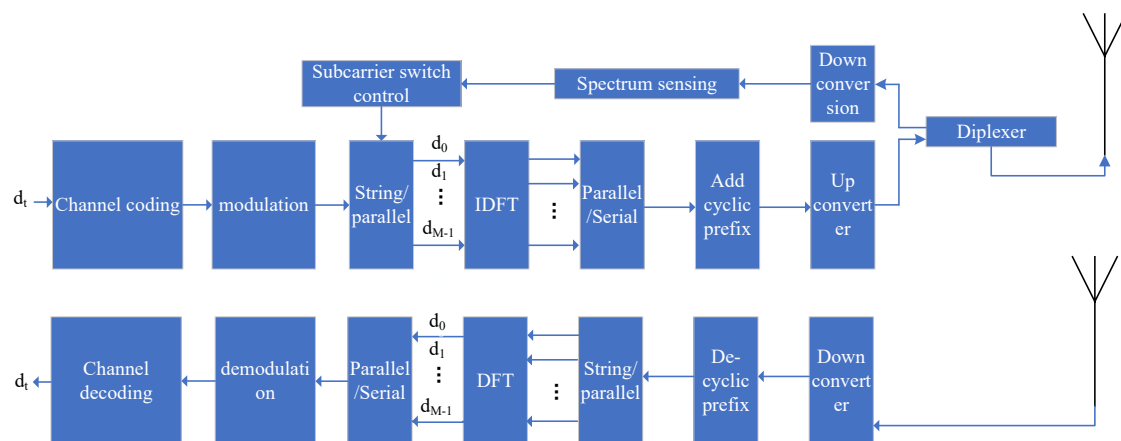


Figure 1. NC-OFDM satellite communication system model based on spectrum sensing.

As shown in Figure 1, the transmit source undergoes channel coding and PSK/QAM modulation, and then it is converted to a set of parallel data d_0, d_1, \dots, d_{M-1} , where M represents the available number of subcarriers in the satellite channel perceived by the spectrum-sensing module. Just like the implementation principle of the OFDM system, the modulation of NC-OFDM can be equivalently realized by Inverse Discrete Fourier Transform (IDFT). The frequencies of the NC-OFDM subcarriers are not continuously distributed because they are determined by the number of spectrum holes and the subcarrier allocation algorithm.

By denoting the number of all subcarriers to be allocated in the satellite channel as N , the NC-OFDM sampling signal can be obtained by N -point IDFT:

$$s_k = \sum_{i \in \{0,1,2,\dots,N-1\}} d_i \exp\left(j \frac{2\pi i k}{N}\right). \quad (1)$$

Similarly, at the receiving terminal, s_k can be inversely transformed to restore the original data d_i :

$$d_i = \sum_{k=0}^{N-1} s_k \exp\left(-j\frac{2\pi ik}{N}\right). \quad (2)$$

3. Compressed Spectrum Sensing

Currently, the frequency range used by one Ku-band communication satellite is about 500 MHz. According to the monitoring results of actual satellite communication frequency occupation, frequency bandwidths of spectrum holes are in the range of about 10 MHz to 100 MHz. Considering the system control complexity brought by the increasing number of subcarriers and the full utilization of spectrum holes, we set the bandwidth of each NC-OFDM subcarrier to 4.125 MHz. So, 500 MHz of bandwidth can be allocated to 122 subcarriers, which include 100 data subcarriers, 12 pilot subcarriers, and 10 protection subcarriers, as shown in Table 1.

Table 1. Subcarriers of Ku satellite with 500 MHz frequency band.

Subcarrier Division Parameters	Definition
number of data subcarriers	100
number of pilot subcarriers	12
number of guard subcarriers	10
total number of subcarriers	122
subcarrier frequency spacing	4.125 MHz

Traditional spectrum sensing methods used for cognitive radio include classic energy detection methods [16], cyclic spectrum estimation [23], etc., but these methods are mainly used for narrowband communication. On the task of simultaneously monitoring all the subchannels among the 500 MHz bandwidth, several challenges arise such as power consumption and cost of high-speed analog-to-digital converters (ADCs). In recent years, compressed sensing has been proposed for broadband spectrum signal monitoring and multiband signal acquisition [24–26]. With a periodic non-uniform sampling framework working far below the Nyquist rate, the signal processing platform based on a software-defined radio can realize real-time, full-band spectrum monitoring within 2 GHz bandwidth, and the spectrum monitoring results can be directly used for spectrum holes extraction and subcarriers allocation.

We hereby propose to integrate the sub-Nyquist sampling and spectrum sensing scheme into the NC-OFDM satellite communication. We adopt a period non-uniform sampling (PNS, also known as Multicoreset sampling) architecture. In the PNS, the baseband signal $x(t)$ is sampled by an interleaved ADC array composed of p low-speed ADCs working under the sampling rate of f_{Nyq}/L , where f_{Nyq} is the Nyquist frequency of the signal and $p < L$. By setting the analog delay in the i -th way as c_i/f_{Nyq} , where c_i is a non-negative integer smaller than L , the sampling sequence in the i -th way can be expressed by Equation:

$$x_i[n] = x\left(\frac{nL}{f_{Nyq}} + \frac{c_i}{f_{Nyq}}\right), n = 1, 2, \dots \quad (3)$$

The i -th way of PNS gives the following measurement:

$$Y_i(f) = \frac{L}{f_{Nyq}} \exp\left(-j2\pi\frac{c_i}{L}f\right) X_i\left(\exp\left(j2\pi f \frac{L}{f_{Nyq}}\right)\right), \quad (4)$$

where $X_i\left(\exp\left(j2\pi f \frac{L}{f_{Nyq}}\right)\right)$ is the discrete time Fourier transform (DTFT) of $x_i[n]$. A linear relationship between the measurement and the original spectrum $X(f)$ is given by Equation (5):

$$y(f) = [Y_1(f)Y_2(f) \dots Y_p(f)]^T, \quad (5)$$

where:

$$x(f) = \left[X\left(f + \frac{(-L/2)f_{Nyq}}{L}\right) X\left(f + \frac{(-L/2+1)f_{Nyq}}{L}\right) \dots \left(f + \frac{(L/2-1)f_{Nyq}}{L}\right) \right]^T \quad (6)$$

and \mathbf{A} is a $p \times L$ matrix with its (i, j) -th element being $a_{i,j} = e^{j2\pi \frac{c}{L}(-2/L+1-1)}$.

The above equation is underdetermined and has infinite solutions. However, by taking advantage of the sparse nature of the spectrum, we can transform the problem into the following l_0 -norm minimization problem:

$$\arg \min_{\hat{\theta}(f) \in \mathbb{C}} |\hat{\theta}(f)|_0 \quad \text{s.t.} \quad |y(f) - \mathbf{A}\hat{\theta}(f)|_2 < \epsilon. \quad (7)$$

This optimization problem is NP-hard but can be approximated by several methods within polynomial time, e.g., convex optimization methods such as basis pursuit (BP), greedy algorithms such as orthogonal matching pursuit (OMP), as well as sparse Bayesian learning algorithm. Among the approaches, greedy algorithms cost far less computation burden than optimization algorithms and yield acceptable solution in high-SNR scenarios. Thus, greedy algorithms, instead of optimization algorithms, are usually adopted in the practical system for better real-time performance. With the above sub-Nyquist sampling and spectrum reconstruction scheme, the average sampling rate acquired by the Ku-band satellites can be significantly reduced.

We used a satellite ground station to monitor a Ku satellite, as shown in Figure 2, and obtained the real star signal spectrum of the satellite in the 500 MHz band range (from 12,300 MHz to 12,800 MHz). The frequency became 1–1.5 GHz after antenna reception and down-frequency conversion amplification (as shown in Figure 3). Six unused spectrum holes were extracted which occupied spectrum band of 296 MHz. Moreover, 69 subcarriers can be allocated in these unused spectra (as shown in Table 2).



Figure 2. The satellite ground station.

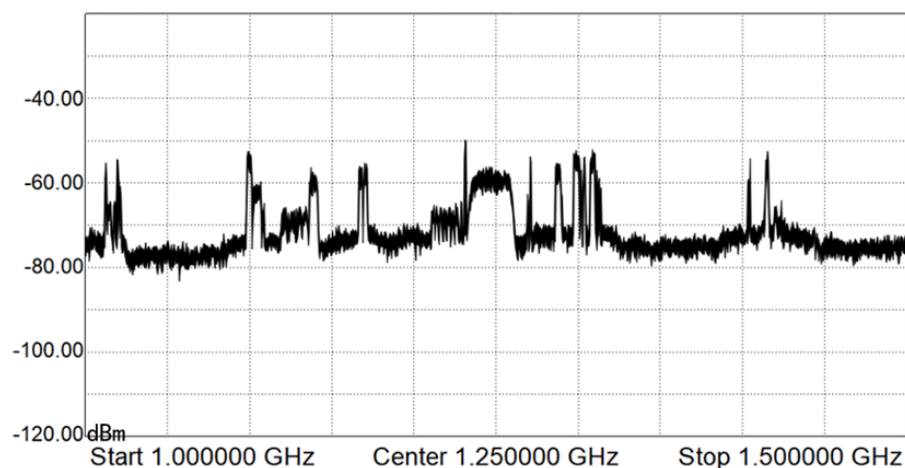


Figure 3. Spectrum sensing results of Ku-band satellite.

Table 2. Spectrum holes extracting and subcarrier allocation.

Spectrum Hole Number	Start Frequency (MHz)	Cut-Off Frequency (MHz)	Bandwidth (MHz)	Assign Sub-Carrier Number
1	12,325	12,395	70	7–23
2	12,445	12,465	20	36–39
3	12,475	12,510	35	43–50
4	12,568	12,582	14	66–68
5	12,615	12,700	85	77–96
6	12,728	12,800	72	106–122

4. Subcarrier Power Allocation Algorithm

NC-OFDM is an unlicensed access system based on cognitive radio. The system needs reasonable resource allocation to maximize the spectrum utilization. Because the bottom noise temperature of each satellite spectrum hole monitored by the spectrum and the sub-carrier channel gain varies, the resource allocation strategy, particularly the power allocation strategy, is a key technology for NC-OFDM cognitive users to achieve high-speed communication.

4.1. The Description of Power Allocation Problem

In these 69 subcarriers, as shown in Table 2, 57 data subcarriers, 6 pilot subcarriers, and 6 protective subcarriers are allocated. According to Figure 3, the noise temperature of each spectrum hole is different, and the difference between the highest and the lowest value is about 6 dB. The demodulation threshold of BPSK modulation plus convolution code used in satellite communication is about 5 to 7 dB. Thus, we set the SNR of NC-OFDM subcarriers as 7–13 dB, as shown in Table 3.

The problem solved by the power allocation algorithm is how to allocate and optimize the subcarrier power to achieve maximum system throughput within limited total power, known occupancy of authorized user frequency bands, and noise temperature constraints. The authors of [27] proposed a distributed power allocation scheme, which is suitable for resource allocation under multi-user and multi-channel conditions, but little consideration is given to the interference problem of authorized users. In [28], a distributed resource allocation scheme was proposed, which proved that the Particle Swarm Optimization (PSO) algorithm and the dual Lagrangian optimization method have similar performance and acceptable computational complexity. The authors of [29] proposed a method of combining the PSO algorithm and the case-based reasoning method for power allocation, which can speed up the convergence, but the case library samples require time and cost accumulation.

In view of the high complexity of the current NC-OFDM sub-carrier power allocation algorithms, a sub-optimal power allocation method based on Hybrid Genetic Particle Swarm Optimization (HGAPSO) algorithm is proposed in this paper.

Table 3. SNR of data subcarriers.

Subcarrier Number	SNR (dB)	Subcarrier Number	SNR (dB)
8	12	67	7
9–19	13	78–79	7
20	13	80–90	10
21	12	91–95	7
22	11	107	7
37	9	108	8
38	8	109	9
44–46	7	110–119	10
47–49	9	120–121	9

The NC-OFDM sub-carrier power allocation scheme is converted into an optimization problem, and the maximum overall throughput of cognitive users in the system is taken as the goal of the optimization. The input optimization algorithm of the power allocation scheme was derived, and the scheme was optimized according to the output analysis of the target. The total number of cognitive users is taken as the optimized objective function according to the transmission rate, which is expressed as Formula (8):

$$\max_{P_i} \sum_{i=1}^N \log_2 \left(1 + \frac{|h_i^{SS}|^2 P_i}{\sigma^2 + J_i} \right). \quad (8)$$

The constraint conditions of the objective function are shown in Equation (9):

$$\sum_{i=1}^N P_i \leq P_{\max}, \sum_{i=1}^N I_i(P_i) \leq I_{th}, \quad (9)$$

where P_i is the power of the i -th sub-carrier, h_i^{SS} is the channel gain coefficient between the subcarriers, and σ^2 is the variance in Gaussian noise. J_i is the interference noise power of the authorized user to the i -th subcarrier:

$$J_i(PU) = \int_{f_i - \Delta f/2}^{f_i + \Delta f/2} \frac{1}{2\pi N} \int_{-\pi}^{\pi} \Phi_{PU}(f) \left(\frac{\sin(\frac{N}{2}(2\pi f - \Phi))}{\sin(\frac{1}{2}(2\pi f - \Phi))} \right) d\Phi, \quad (10)$$

where $\Phi_{PU}(f)$ is the power spectral density function of the authorized user, f_i is the center frequency of the authorized user, and Δf is the bandwidth of the cognitive user. The interference power brought by cognitive users to authorized users is shown in Equation (11):

$$I_i(P_i) = P_i |h^{SP}|^2 T_s \int_{f_i - B_p/2}^{f_i + B_p/2} \left(\frac{\sin(\pi f T_s)}{\pi f T_s} \right)^2 df, \quad (11)$$

where B_p is the bandwidth of the authorized user, and h^{SP} is the channel gain coefficient introduced by the cognitive user to the authorized user.

4.2. Hybrid Genetic Particle Swarm Optimization Algorithm for Power Distribution

Power allocation can be solved by using an optimization algorithm, and the design of the algorithm is the key to the overall performance of cognitive users. At present, optimiza-

tion algorithms are widely studied, including Genetic Algorithms (GA), PSOs, simulated annealing algorithms, tabu search algorithms, differential evolutionary algorithms, etc., among which GAs and PSOs are the two most widely used algorithms. GAs are a kind of random optimization search method based on the evolutionary rules of the biological world. They can use the search information of multiple search points at the same time. They have the characteristics of parallel operation and are suitable for large-scale complex optimization problems. The factor that has an impact on fitness is the subcarrier power. Therefore, the subcarrier power sequence is adopted as the chromosome in a GA. When the fitness function meets the output requirements, the algorithm outputs the sub-optimization results through initialization, coding, selection, crossover, compilation, and other basic operations.

The idea of the GA comes from natural selection theory, and it has certain advantages for obtaining the optimal solution by searching for the most eligible individuals in the global space based on the rules of survival of the fittest. From the perspective of evolutionary iterations, the PSO algorithm makes use of the information interaction and individual memory within the population to speed up the search. In this paper, combined with the advantages of the two algorithms, a hybrid genetic particle swarm optimization algorithm is proposed. The evolutionary idea of the PSO algorithm is integrated into the updated GA, and the algorithm optimization is achieved by using the competition between the two algorithms.

The flow and update process of the HGAPSO algorithm are shown in Figures 4 and 5, respectively.

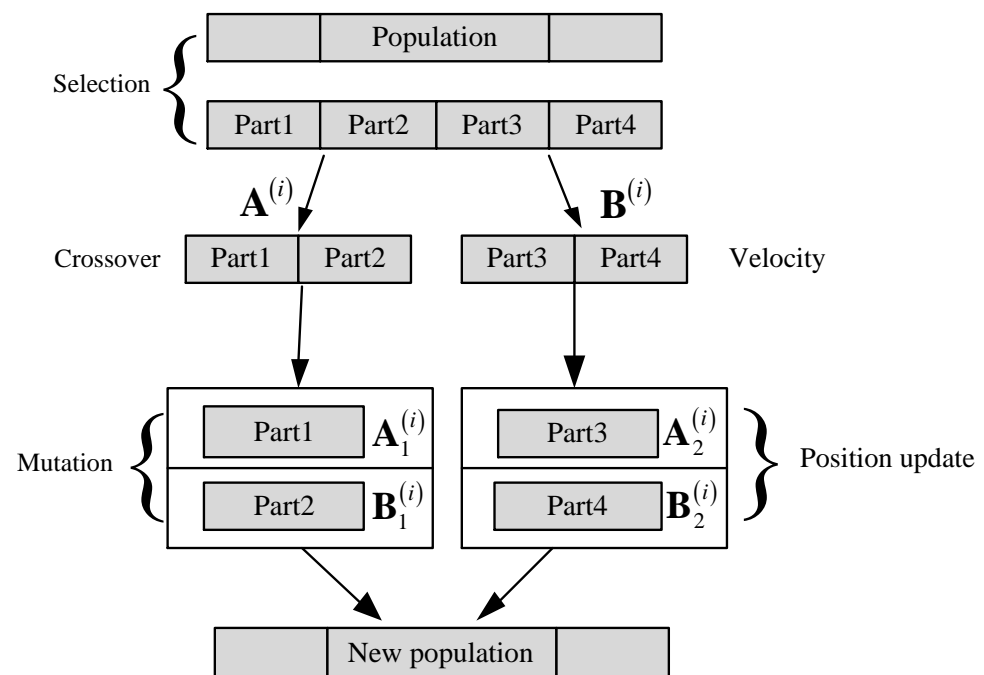


Figure 4. The flow of the HGAPSO.

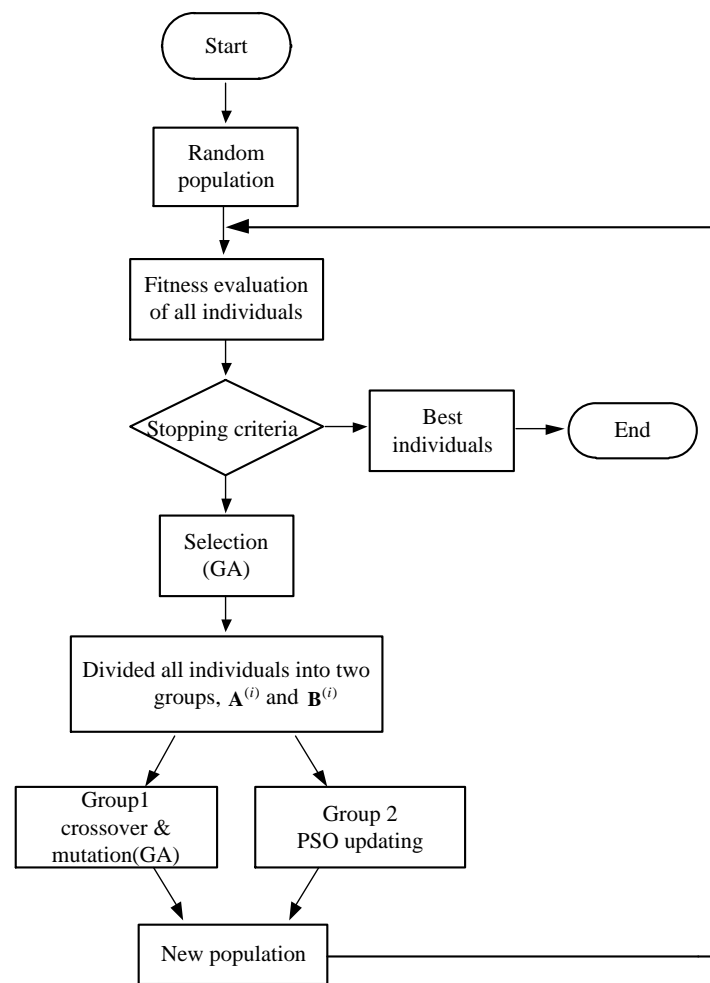


Figure 5. Optimization process of the HGAPSO algorithm.

The specific optimization steps of HGAPSO are shown in Algorithm 1.

Algorithm 1 HGAPSO.

- 1: Set particle update speed, population size, number of particles, weight factor c_1 , weight factor c_2 , coding method, crossover probability, mutation probability;
 - 2: Generate a population randomly, initialize particle position, particle speed, and calculate its fitness;
 - 3: In the population, find the global best and the best individual and calculate the corresponding best fitness value; randomly divide the population into two categories, defined as $\mathbf{A}^{(i)}$ and $\mathbf{B}^{(i)}$;
 - 4: For each group, it is divided into two groups according to the degree of fitness, one of which has a fitness greater than two. Among them, form a new population using GA for crossover and mutation operations; $\mathbf{A}_2^{(i)}$ and $\mathbf{B}_2^{(i)}$ form another population, using PSO algorithm to update particle speed and position;
 - 5: Form a new population after completing the update together, and recalculate the fitness value;
 - 6: Judge whether the optimal population meets the requirements or not, then return to step 4, and output the result if it is satisfied.
-

4.3. Analysis of Algorithm Performance

In order to analyze the performance of optimal algorithms for power allocation, 2000 Monte Carlo simulations were conducted for each algorithm. Assuming that the

simulation scenario contains 10 cognitive users and 1 authorized user, the signal-to-noise ratio (SNR) of the channel is 0 dB. In order to ensure that each iteration operation time of the three algorithms is similar, the parameters adopted in the simulation are shown in Table 4.

Table 4. Parameters of different algorithms.

Algorithm	Parameters
GA	Evolutionary algebra: 200, population size: 300, crossover probability: 0.3, mutation probability: 0.05
PSO	Number of iterations: 200, population size: 60, particle speed: 2, weight factor c_1 : 0.5, weight factor c_2 : 1.5
HGAPSO	Evolutionary algebra: 200, population size: 100, particle velocity: 2, weight factor c_1 : 0.5, weight factor c_2 : 1.5, crossover probability: 0.3, mutation probability: 0.05

Figure 6 shows the system throughput changes generated by iterative operation simulation using three algorithms. As can be seen from the comparison of curves in Figure 6, the HGAPSO algorithm achieves the highest system throughput under the same number of evolution, followed by GA, and the PSO algorithm has the worst performance. After hundreds of iterations, the three algorithms converge on their best performances, among which, the peak throughput of the HGAPSO algorithm is 5.325 Mbps, and that of the GA and PSO are 5.077 and 4.496, respectively. This result shows that under the same evolutionary algebra and complexity, the HGAPSO power allocation algorithm achieves the maximum cognitive user throughput, which is improved by 4.88% and 18.44%, respectively, compared with the GA and the PSO algorithm.

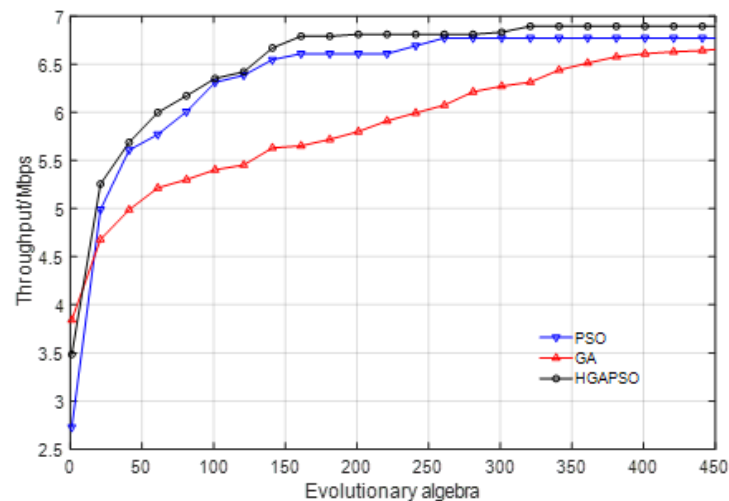


Figure 6. Comparison of the throughput by different algorithms.

5. Simulation of NC-OFDM Satellite Communication System

5.1. BER Performance of NC-OFDM Satellite Communication System

In order to avoid interference from the subcarrier side band to the adjacent frequencies of authorized users, a frequency domain filter is applied before emission on each subcarrier signal. The spectrum of the IF signal composed of 57 data subcarriers is shown in Figure 7.

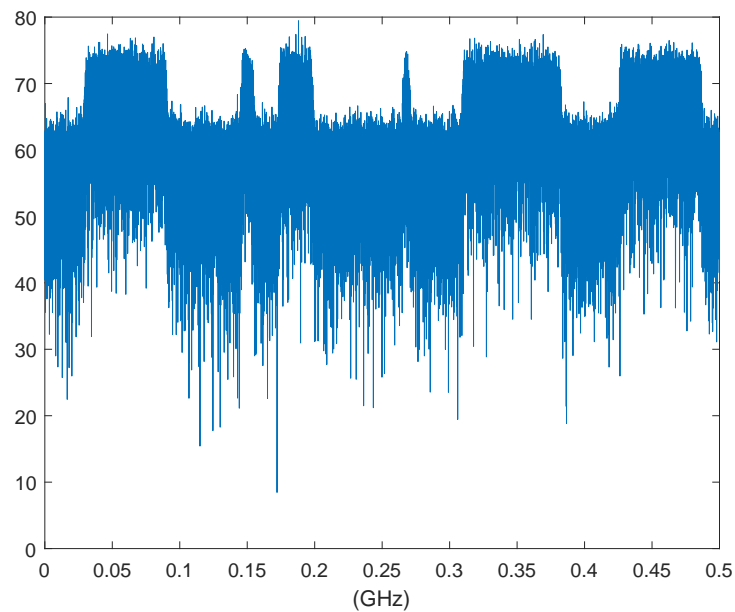


Figure 7. Spectrum of data subcarriers of NC-OFDM.

The channel coding adopts convolutional code 2,1,6, and the modulation type is BPSK. The transmission and reception of all data subcarriers are simulated and the BER performance is obtained as shown in Figure 8.

The BER threshold of satellite communication is usually 10^{-3} – 10^{-4} . As shown in Table 4, 11 subcarriers do not meet the requirements. The reason is that their frequencies are at the up and down boundary of the entire data subcarrier frequency domain, which cannot offset the interference of subcarriers efficiently as OFDM. It can be seen that 57 effective data subcarriers realize a data transmission rate of 228 Mbps, which proves that the NC-OFDM system can make efficient use of the spectrum holes in satellite communication.

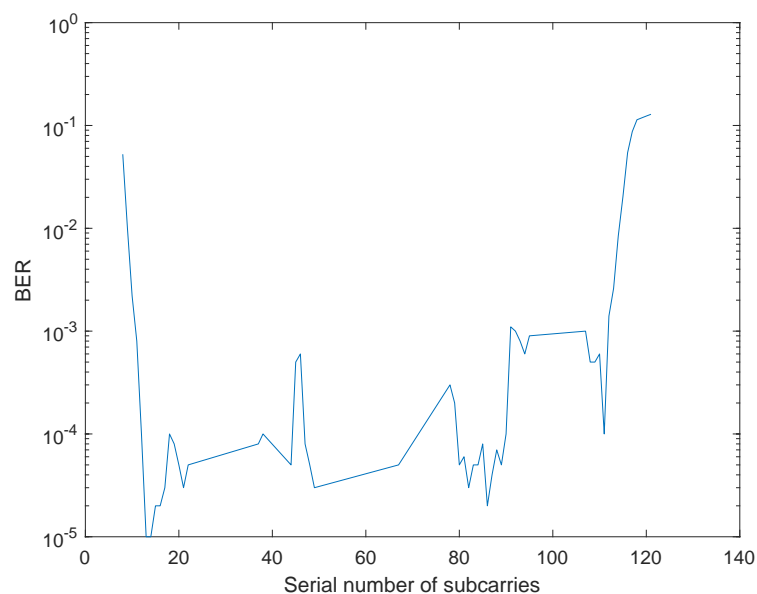


Figure 8. BER of data subcarriers of NC-OFDM.

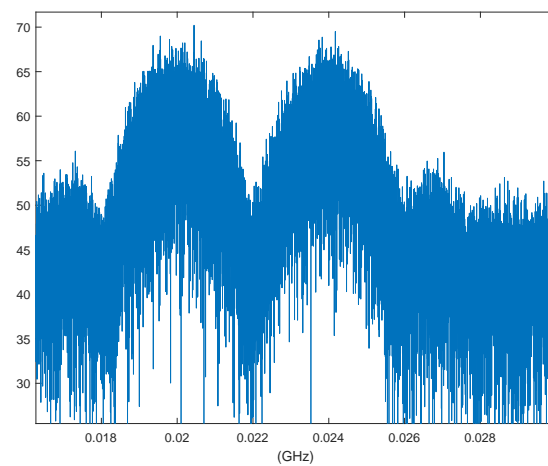
5.2. Interference Analysis of NC-OFDM Signal to Authorized Signal

The Spectrum Overlap Ratio (SOR) ΔF is defined as the ratio of the spectrum overlapping range between an authorized signal and an NC-OFDM signal to the frequency bandwidth of the former. We suppose that the carrier frequency of the authorized signal is

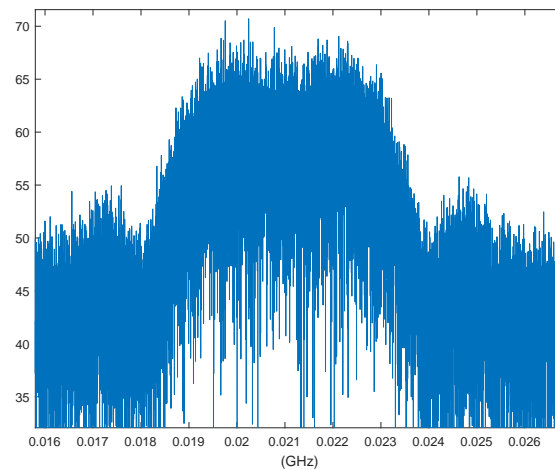
f_{c1} , the code rate is f_{d1} , the carrier frequency of the adjacent NC-OFDM subcarrier is f_{c2} , and the code rate is f_{d2} , and they all use MPSK modulation. Therefore:

$$\Delta F = \frac{f_{d1} + f_{d2} - |f_{c1} - f_{c2}|}{2f_{d1}} \quad (12)$$

We assume that the NC-OFDM signal can make full use of the subchannel gain and the power spectrum densities of subcarriers approach to authorized signal, and both the modulation rate of the authorized signal and the NC-OFDM subcarrier rate are 4MBD. When ΔF equals 0 and 50%, the spectrum of the authorized signal and the adjacent NC-OFDM subcarrier are shown in Figure 9.



(a)



(b)

Figure 9. Spectra of QPSK authorized signal and adjacent subcarrier of NC-OFDM: (a) Spectrum with $\Delta F = 0$; (b) Spectrum with $\Delta F = 50\%$.

Under the conditions of ΔF as 0, 25%, 37.5%, and 50% respectively, the reception BER results of authorized signal with BPSK modulation and convolution coding are shown in Figure 10.

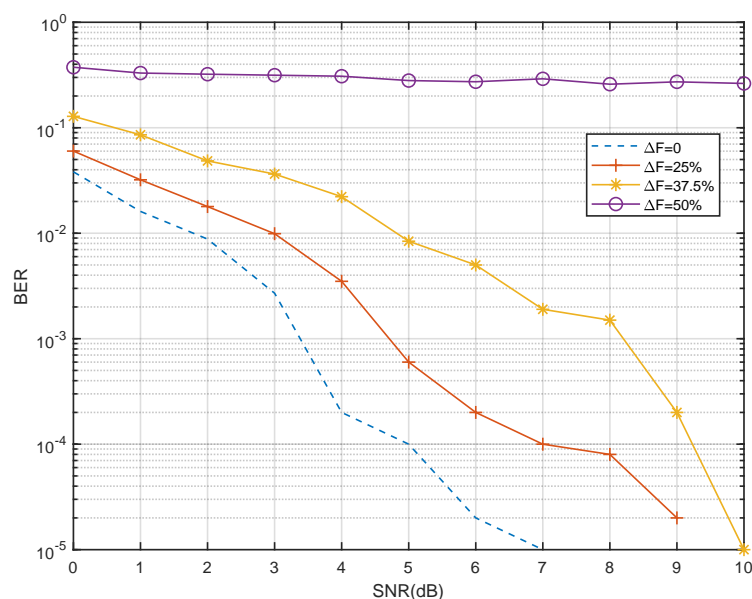


Figure 10. BER of authorized signal with NC-OFDM interference.

6. Conclusions

NC-OFDM communication has advantages of flexible and controllable subcarriers, and it is a promising technique to improve satellite communication spectrum efficiency. The key issue of whether NC-OFDM can be applied is its compatibility with authorized satellite communication users.

Based on the compressed spectrum sensing of a real satellite channel, a subcarrier distribution scheme for NC-OFDM satellite communication is proposed in this paper. Moreover, a hybrid genetic particle swarm optimization algorithm is proposed for NC-OFDM sub-carrier power control, which maximizes the throughput of the NC-OFDM system. Through the effective utilization of the satellite spectrum holes, the extra data transmission of 228 Mbps is achieved, which is impressive for commercial communication satellites with a bandwidth of 500 MHz. The concept of the spectrum overlap ratio is defined to describe the interference of NC-OFDM signals to authorized signals. The BER performance of authorized system under interference condition is studied. Fast and efficient spectrum sensing and flexible power allocation of subcarriers are effective ways to solve the compatibility problem. The NC-OFDM satellite communication method can significantly improve the spectrum efficiency of satellite communication. This work is an extended version of the previously published conference paper [22].

Author Contributions: Writing—original draft preparation, Y.W., Q.Z. and L.W.; writing—review and editing, H.N.; supervision, Y.G.; funding acquisition, Z.L. All authors have read and agreed to the published version of the manuscript.

Funding: This research was funded by the National Natural Science Foundation of China (61901490 and 61671454) and the Research Plan Project of NUDT (ZK21-33).

Conflicts of Interest: The authors declare no conflict of interest.

References

1. Mitola, J.; Maguire, G. Cognitive radio: Making software radios more personal. *IEEE Pers. Commun.* **2019**, *6*, 13–18. [[CrossRef](#)]
2. Haykin, S. Cognitive radio: Brain-empowered wireless communications. *IEEE J. Sel. Areas Commun.* **2005**, *23*, 201–220. [[CrossRef](#)]
3. Jamoos, A.; Abdou, A. Spectrum measurements and analysis for cognitive radio applications in palestine. In Proceedings of the 2019 6th International Conference on Electrical and Electronics Engineering (ICEEE), Istanbul, Turkey, 16–17 April 2019; pp. 180–185.
4. Lin, Z.; Niu, H.; An, K.; Wang, Y.; Zheng, G.; Chatzinotas, S.; Hu, Y. Refracting RIS aided hybrid satellite-terrestrial relay networks: Joint beamforming design and optimization. *IEEE Trans. Aerosp. Electron. Syst.* **2022**, *1*. [[CrossRef](#)]

5. Lin, Z.; Lin, M.; de Cola, T.; Wang, J.-B.; Zhu, W.-P.; Cheng, J. Supporting IoT with rate-splitting multiple access in satellite and aerial-integrated networks. *IEEE Internet Things J.* **2021**, *8*, 11123–11134. [[CrossRef](#)]
6. Lin, Z.; Lin, M.; Wang, J.-B.; de Cola, T.; Wang, J. Joint beamforming and power allocation for satellite-terrestrial integrated networks with non-orthogonal multiple access. *IEEE J. Sel. Top. Signal Process.* **2019**, *13*, 657–670. [[CrossRef](#)]
7. Lin, Z.; Lin, M.; Champagne, B.; Zhu, W.-P.; Al-Dhahir, N. Secure and energy efficient transmission for RSMA-based cognitive satellite-terrestrial networks. *IEEE Wirel. Commun. Lett.* **2021**, *10*, 251–255. [[CrossRef](#)]
8. Lin, Z.; Lin, M.; Champagne, B.; Zhu, W.-P.; Al-Dhahir, N. Secure beamforming for cognitive satellite terrestrial networks with unknown eavesdroppers. *IEEE Syst. J.* **2021**, *15*, 2186–2189. [[CrossRef](#)]
9. Lin, Z.; Lin, M.; Wang, J.-B.; Huang, Y.; Zhu, W.-P. Robust secure beamforming for 5G cellular networks coexisting with satellite networks. *IEEE J. Sel. Areas Commun.* **2018**, *36*, 932–945. [[CrossRef](#)]
10. Lin, Z.; Lin, M.; Champagne, B.; Zhu, W.-P.; Al-Dhahir, N. Secrecy-energy efficient hybrid beamforming for satellite-terrestrial integrated networks. *IEEE Trans. Commun.* **2021**, *69*, 6345–6360. [[CrossRef](#)]
11. An, K.; Lin, M.; Ouyang, J.; Zhu, W.-P. Secure transmission in cognitive satellite terrestrial networks. *IEEE J. Sel. Areas Commun.* **2016**, *34*, 3025–3037. [[CrossRef](#)]
12. An, K.; Liang, T.; Zheng, G.; Yan X.; Li, Y.; Chatzinotas, S. Performance limits of cognitive-uplink FSS and terrestrial FS for Ka-band. *IEEE Trans. Aerosp. Electron. Syst.* **2019**, *55*, 2604–2611. [[CrossRef](#)]
13. Guidotti, A.; Vanelli-Coralli, A.; Conti, M. Facilitating opportunities for flexible, efficient, and reliable spectrum use employing cognitive radio technologies. *NPRM Order ET Docker* **2003**, *03-108*, FCC03-322.
14. Rajbanshi, R.; Wyglinski, A.M.; Minden, G.J. An efficient implementation of NC-OFDM transceivers for cognitive radios. In Proceedings of the 1st International Conference on Cognitive Radio Oriented Wireless Networks and Communications, Mykonos, Greece, 8–10 June 2006; pp. 4–5.
15. Van, J.; Berggren, F. N-continuous OFDM. *IEEE Commun. Lett.* **2009**, *13*, 1–3.
16. Shamani F.; Airoidi R.; Sevom, V.F.; Ahonen, T.; Nurmi, J. FPGA implementation issues of a flexible synchronizer suitable for NC-OFDM-based cognitive radios. *J. Syst. Archit.* **2017**, *76*, 102–116. [[CrossRef](#)]
17. Ma, D.; Shi, Y.; Zhang, W.; Guozhen, L. Design of acoustic transmission along drill strings for logging while drilling data based on adaptive NC-OFDM. *Aeu Int. J. Electron. Commun.* **2017**, *83*, 329–338. [[CrossRef](#)]
18. Liu, X.; Zhang, L.; Xiong, J.; Zhang, X.; Zhou, L.; Wei, J. Peak-to-average power ratio analysis for OFDM-based mixed-numerology transmissions. *IEEE Trans. Veh. Technol.* **2020**, *69*, 1802–1812. [[CrossRef](#)]
19. Na, Z.; Guan, Q.; Fu, C.; Cui, Y.; Guo, Q. Channel model and throughput analysis for LEO OFDM satellite communication system. *Int. J. Future Gener. Commun. Netw.* **2013**, *6*, 109–112. [[CrossRef](#)]
20. Shirmohammadi, M.; Damavandi, A. Blind channel estimation of MIMO-OFDM systems in satellite communication. In Proceedings of the 2015 International Conference on IEEE Information and Communication Technology Convergence (ICTC), Jeju Island, Korea, 28–30 October 2015; pp. 704–709.
21. Bai, X.; Zhu, W.; Liu, B. A Ku band satellite spectrum signal detection method based on bottom noise fitting. *J. Nanjing Univ. Posts Telecommun. (Nat. Sci. Ed.)* **2019**, *39*, 51–57.
22. Wang, Y.; Zhao, Q.; Ma, S.; Jiang, Y.; Wang, L. Satellite communication based on non-continuous orthogonal frequency division multiplexing. In Proceedings of the 2020 IEEE 20th International Conference on Communication Technology (ICCT), Nanning, China, 28–31 October 2020; pp. 638–642.
23. Qi, Y.; Tao, P.; Qian, R.; Rongrong, Q. Cyclostationarity-based spectrum sensing in cognitive radio. *J. Nanjing Univ. Posts Telecommun. (Nat. Sci. Ed.)* **2009**, *21*, 353–357.
24. Yang, J.; Song, Z.; Gao, Y.; Gu, X.; Feng, Z. Adaptive compressed spectrum sensing for multiband signals. *IEEE Trans. Wirel. Commun.* **2021**, *14*, 7642–7654. [[CrossRef](#)]
25. Song, Z.; Gao, Y.; Tafazolli, R. A survey on spectrum sensing and learning technologies for 6G. *IEICE Trans. Commun.* **2021**, *104*, 1207–1216. [[CrossRef](#)]
26. Song, Z.; Qi, H.; Gao, Y. Real-time multi-gigahertz sub-Nyquist spectrum sensing system for mmwave. In Proceedings of the 3rd ACM Workshop on Millimeter-Wave Networks and Sensing Systems, Los Cabos, Mexico, 25 October 2019; pp. 33–38.
27. Barbarossa, S.; Sardellitti, S.; Scutari, G. Joint optimization of detection thresholds and power allocation for opportunistic access in multicarrier cognitive radio networks. In Proceedings of the 2009 3rd IEEE International Workshop on Computational Advances in Multi-Sensor Adaptive Processing (CAMSAP), Aruba, Netherland Antilles, 13–16 December 2009.
28. Ma, N.; Yang, M.; Shin, Y. A distributed power allocation algorithm for OFDM-based cognitive radio networks. In Proceedings of the 2013 IEEE International Conference of IEEE Region 10 (TENCON 2013), Xi'an, China, 22–25 October 2013.
29. Zhan, W.; Zhou, X.; Liu, Y. Radio resource allocation based on case-reasoning in NC-OFDM systems for cognitive radio. *Mob. Commun.* **2017**, *41*, 82–88.